ELSEVIER

Journal of Alloys and Compounds 317–318 (2001) 39–43

Journal of ALLOYS AND COMPOUNDS

www.elsevier.com/locate/jallcom

Single crystal neutron diffraction investigations of the crystal and magnetic structures of $R_2Fe_{14}B$ (R=Y, Nd, Ho, Er)

P. Wolfers*, M. Bacmann, D. Fruchart

Laboratoire de Cristallographie, CNRS, 25 Avenue des Martyrs, BP 166, 38042 Grenoble Cedex 9, France

Abstract

The compounds of general formula $R_2Fe_{14}B$ form a series of magnetic materials, the prototype of which, $Nd_2Fe_{14}B$, is used to make high performance permanent magnets. These compounds crystallise in the tetragonal space group $P4_2/mnm$ and with R=Nd, Ho, Er, Tm and Yb a spin reorientation transition was found. Precise structural analyses using neutron diffraction on single crystals were undertaken. It is clearly demonstrated that lowering of symmetry takes place for non-axial compounds. Besides, large deviations to collinearity of the magnetic arrangements were determined. © 2001 Elsevier Science B.V. All rights reserved.

Keywords: Neutron diffraction; Crystallographic structure; Magnetic structure

1. Introduction

The compounds of general formula $R_2Fe_{14}B$ form a series of anisotropic ferromagnetic materials used worldwide to make high performance permanent magnets. The crystal structure of the series was described in the tetragonal space group $P4_2/mnm$ [1–3]. Several types of magnetic behaviour were observed (Fig. 1) [3]: (1) easy axis compounds, where the magnetisation is aligned along the *c*-axis; (2) easy plane compounds where the magnetisation lies within the (*a*, *b*) plane, at low temperature, (3) and more complex cases of $Nd_2Fe_{14}B$ and $Ho_2Fe_{14}B$ where the magnetisation rotates continuously from the *c*-axis to a tilted direction in the (110) plane (Fig. 1).

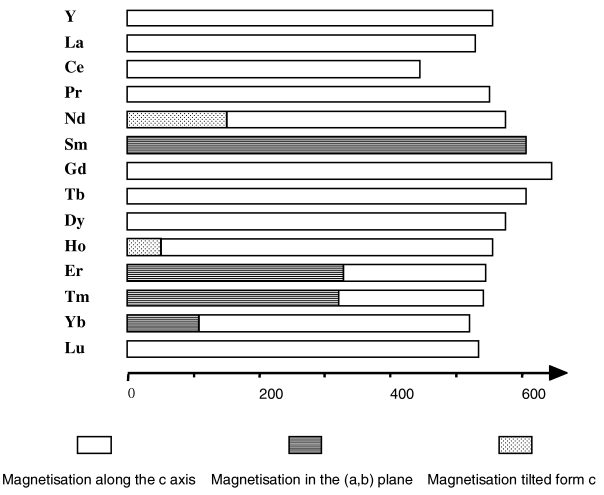

Fig. 1. Magnetisation orientations in the $R_2Fe_{14}B$ series [3].

Some compounds present a first order transition that takes place between the low temperature easy plane and the high temperature easy axis states (R=Er, Tm, Yb). For the Sm compound, no such transition was found since it orders easy plane up to the ferro-paramagnetic transition at $T_c \approx 580$ K.

These spin rotations were attributed to the competition between iron and rare-earth magnetic sublattice anisotropies. The purpose of this study was to determine accurately the low temperature crystal and magnetic structures in order to better understand the spin rotation mechanisms.

To get a reliable picture of the whole series, taking in account the single crystal availability, we selected the R=Ho, Nd, Er and Y (pure easy axis material) compounds.

2. Neutron diffraction experiments

Table 1 displays the samples and instrument characteristics we used to perform the neutron diffraction measurements: the single crystals were grown by the Czochralski method and cut as spheres by spark erosion. Prior to performing the four-circle neutron diffraction analysis, the neutron Laue technique was used both for checking the

*Corresponding author. Tel.: +33-76-887-405; fax: +33-76-881-038.

0925-8388/01/$ – see front matter
PII: S0925-8388(00)01353-0

Table 1
Diffraction data of $Ho_2Fe_{14}B$, $Nd_2Fe_{14}B$, $Er_2Fe_{14}B$ and $Y_2Fe_{14}B$

Compound		$Ho_2Fe_{14}B$		$Nd_2Fe_{14}B$	$Er_2Fe_{14}B$	$Y_2Fe_{14}B$
Crystal diameter		1.6 mm		2.2 mm	2.0 mm	2.0 mm
Instrument		D9		D10	D9	D9
Cooling system		Refrigerator		He cryostat	Refrigerator	Refrigerator
Wavelength		0.85 Å		1.26 Å	0.84 Å	0.84 Å
Counter type		Single		Single	32×32 cells	32×32 cells
Temperature	300 K	100 K	20 K	20 K	20 K	20 K
Intensity number	388	793	1927	452	1411[a]	3454[a]
Fit. variable number	27	88	88	68	76	30
Crystal Φ (mm)		1.6		2.2	2.0	1.8
Space group	$P4_2/mnm$	Cm	Cm	Cm	$Pnn2$	$P4_2/mnm$
Domain weight (%)						
W_1		25.6(9)	25.9(5)	1/4	24(2)	
W_2		25.9(8)	25.3(5)	1/4	23(2)	
W_3		21.9(9)	23.4(5)	1/4	23(2)	
W_4		26.6(8)	25.4(5)	1/4	29(2)	
Scale factor	0.918(8)	5.49(5)	5.55(5)	20.5(2)	0.310(1)	0.303(1)
Extinction coeff.	0.20(1)	0.22(2)	0.27(1)	0.3(1)	0.174(2)	0.24(1)
Goodness of fit χ^2	3.1	1.22	1.90	1.90	10.21	1.76
R factor (%)	4.25	3.79	6.01	4.71	4.47	4.84

[a] Use all measured reflections in the half reciprocal space (crystal was an approximate sphere).

crystal quality and to orient the sample on a dedicated pinhole.

3. Data collection and structure determination management

The different steps of the data management were as follows.

1. A *peak integration* was performed using the data reduction system of the ILL programs Library: COLL5 for Ho and Nd, SCATER for Er and Y compounds. This procedure was made independent of any particular data interpretation and provides a first estimation of the intensity and the standard deviation of each line.
2. An *absorption correction* adapted for a spherical crystal was applied using Dwigging's table [4]. For this correction the cross-sections of the elements were estimated by extrapolation to the wavelength used of the data given by the BNL charts [5]. Furthermore, experimental determinations of the transmission factors agree with the theoretical one within 1%.
3. The *equivalent reflections* of each of the tried space groups were substituted by their average value in order to build inequivalent symmetry data sets.
4. For a given space group G (i.e. a given subgroup of $Ga = P4_2/mnm$ already reported) the sample was assumed to be twinned. Each of the elementary domains was deduced from the 'theoretical' single crystal sample by application of a factor group F. This factor group is the symmetry group that generates the tetragonal space group Ga from the single crystal space group G: $Ga = G \otimes F$. So, each of the diffraction lines is the sum of the lines issued from the twins deduced by the application of the factor group. For example, if $G = Cm$, $F = 4/m$ in order to generate the full orientation group $4/mmm$ (corresponding to the space group $P4_2/mnm$). Hence, the sample volume is described by an eight-domain twinning. Using neutron diffraction, the nuclear structure factors are quasi-real quantities since the imaginary part of the Fermi lengths (boron only) is negligible. Thus Friedel's rule is well applied and we can keep only four twin partners. Each reflection intensity is computed as the sum of each twin partner contribution (with a related weight). Fig. 2 displays the case of $Nd_2Fe_{14}B$.

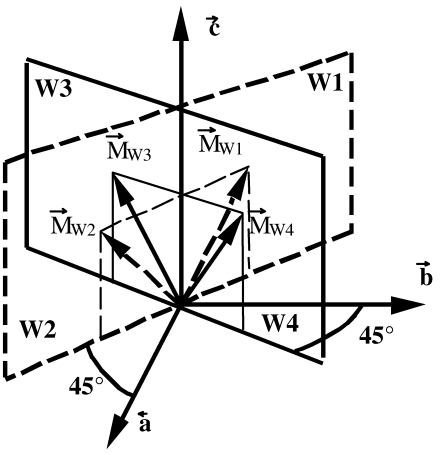

$$I(\vec{h}) = \sum_{f \in F} w_f \cdot I(f \otimes \vec{h})$$

Fig. 2. Domains in a crystal of $Ho_2Fe_{14}B$ (with $Ga = P4_2/mnm$, $G = Cm$, $F = 4$). w_f and i_f denote the relative weights and reflection intensity of the fth twin partner where f is an element of F.

5. A *secondary extinction* effect was considered as non-negligible, since strong reflections are found attenuated by 25%. The Becker and Coppens' secondary extinction formalism was applied for a crystal 'type I' and a Lorentzian mosaic distribution [6]. A valuable correction was obtained when the extinction formula was applied to the sum of the nuclear and magnetic squared structure factors.
6. The structure factor calculations were performed by using the scattering lengths of the elements compiled by Sears [7], and the magnetic form factors compiled by Brown [8].
7. No correction for harmonic wavelengths was applied due to the weakness of the ratio:

$$I(\lambda/2)/I(\lambda) \leq 5 \times 10^{-4}.$$

The points 4 to 7 were carried out during the crystallographic least-squares process using the program MXD [9].

Starting from space group $P4_2/mnm$, the structure was described using the Shoemaker's atom site notations [1].

The strategy used for managing the least-squares refinements was not obvious. Since the domain weights are nearly equivalent quantities, the variations of diffraction line intensities are weak. The structure factor first order terms appear quasi-negligible, but the second order terms (quadratic) are of reasonable strength and they compete with the thermal factors (Debye–Waller) and the magnetic contributions (decreasing with scattering vector **h**). In order to minimise possible correlation effects, we have in parallel:

- forced all the magnetic iron moments to be antiparallel (Ho and Er) and parallel (Nd) to the resulting sum of the rare-earth moments;
- introduced progressively selected low temperature space group constraints, substituting $P4_2/mnm$, when (reference to the e.s.d.) the observed deviations from the higher symmetry were found significant.

4. Main results

The crystal structures analysed from the room temperature data collection are all in good agreement with the results already published [1,2].

The room temperature magnetic structures are all collinear, and for R=Y, Nd, Ho, the resulting magnetisations are parallel to the *c*-axis. This is also the case for $Y_2Fe_{14}B$ at all temperatures. No symmetry lowering was detected for this compound even at low temperature, contrarily to the other three compounds for which it was necessary to describe the crystal symmetry in an orthorhombic (Er) and a monoclinic (Nd and Ho) subgroup. Then, we will detail more particularly the two types of behaviour — Nd and Ho on a side, Er on the other side — with brief references to physical characteristics.

4.1. $Nd_2Fe_{14}B$ and $Ho_2Fe_{14}B$ [10–13]

The $Nd_2Fe_{14}B$ and $Ho_2Fe_{14}B$ compounds exhibit continuous spin reorientation phenomena below $T_{SR}=140$ and 58 K, respectively. Magnetisation measurements show that the low temperature easy direction is tilted from the tetragonal axis in the (110) plane [3]. In the present study the forbidden reflections $h0l$ and $0kl$ with odd $h+l$ or $k+l$ values were observed at all temperatures, including room temperature. The main result of our analysis is that a lower symmetry, space group Cm', appears far above the spin reorientation temperature. However, at room temperature the previously reported tetragonal symmetry, space group $P4_2/mnm$, can be regarded as a not so bad approximation. High magnetostrictive forces can generate such a crystal and magnetic symmetry lowering.

The complete structure description of $Nd_2Fe_{14}B$ and $Ho_2Fe_{14}B$ were reported in Refs. [10–13].

4.2. $Er_2Fe_{14}B$

The low temperature data revealed itself to be not compatible with the $P4_2/mnm$ space group. The space

Table 2
Magnetic structures of $Ho_2Fe_{14}B$, $Nd_2Fe_{14}B$, $Er_2Fe_{14}B$ and $Y_2Fe_{14}B$. Magnetisation and iron moment orientations

Compound		$Ho_2Fe_{14}B$			$Nd_2Fe_{14}B$	$Er_2Fe_{14}B$	$Y_2Fe_{14}B$
Temperature	K	300	100	20	20	20	20
M(Re 4*f*)	μ_B	−5.79(8)	−8.89(6)	−10.00(5)	3.20(7)	−9	
M(Re 4*g*)	μ_B	−5.74(7)	−9.17(6)	−10.00(5)	3.21(5)	−9	
Fe θ	°	0	4(1)	23(1)	33.3(8)	90	0
Fe φ	°		45	45	45	0	
M(Fe1 — 4*c*)	μ_B	2.07(7)	2.43(5)	2.53(4)	2.69(1)	2.41(4)	2.44(10)
M(Fe2 — 16*k*)	μ_B	2.23(7)	2.58(4)	2.45(3)	2.39(6)	2.63(3)	2.60(07)
M(Fe3 — 16*k*)	μ_B	2.07(6)	2.52(4)	2.50(4)	2.28(7)	2.59(3)	2.64(06)
M(Fe4 — 8*j*)	μ_B	2.75(9)	3.08(5)	3.08(5)	2.75(1)	2.94(3)	3.09(07)
M(Fe5 — 8*j*)	μ_B	1.88(8)	2.31(5)	2.21(4)	2.07(8)	2.15(3)	2.33(08)
M(Fe6 — 4*e*)	μ_B	2.00(8)	2.50(5)	2.31(4)	2.22(1)	2.31(6)	2.71(11)
Magnetisation	μ_B	19(1)	18.5(5)	15.5(5)	38.75(1)	18.5(2)	36.95(50)
θ (M)	°	0	4.0(5)	22.5(5)	32.6(8)	90	0
φ (M)	°		45	45	45	0	0

Table 3
Magnetic structures of $Ho_2Fe_{14}B$, $Nd_2Fe_{14}B$ and $Er_2Fe_{14}B$. Orientations of the rare earth moments

	$Ho_2Fe_{14}B$ 100 K		$Ho_2Fe_{14}B$ 20 K		$Nd_2Fe_{14}B$ 20 K		$Er_2Fe_{14}B$ 20 K	
	$\theta°$	$\phi°$	$\theta°$	$\phi°$	$\theta°$	$\phi°$	$\theta°$	$\phi°$
Position 4*f*								
Site 1	8(3)	45	18(1)	45	47(6)	45	94.2(1.8)	−15.9(0.5)
Site 2	−4(3)	45	22(1)	45	12(3)	45	81.5(1.5)	−1.7(0.6)
Site 3	2(1)	−59(35)	21(1)	9(2)	38(3)	98(3)	85.8(1.8)	15.9(0.5)
Site 4	2(1)	149(35)	21(1)	81(2)	38(3)	−8(3)	98.5(1.5)	1.7(0.6)
Position 4*g*								
Site 1	8(3)	−59(35)	24(1)	89(2)	66(3)	69(4)	97.7(1.5)	22.6(0.5)
Site 2	8(3)	149(35)	24(1)	1(2)	66(3)	−21(4)	83.5(1.5)	11.0(0.5)
Site 3	−4(4)	45	29(1)	45	−9(4)	45	82.3(1.5)	−22.6(0.5)
Site 4	2(1)	45	33(1)	45	50(5)	45	96.5(1.5)	−11.0(0.5)

group *Pn′n2′* was retained as compatible both with the easy magnetisation direction [100] and the extinction of the reflections *h*0*l* and 0*kl* (odd values of $h + l$ and $k + l$). The results of the fits clearly indicate that neither the magnetic structure remains collinear, nor the crystal structure remains tetragonal.

Tables 1–3 give the crystal and magnetic structure parameters and some other relevant quantities.

5. Discussion

The low temperature crystal and magnetic structures (Fig. 3) of the $R_2Fe_{14}B$ exhibiting spin reorientation transition (SRT) must be related to the competing parameters, exchange and magnetostrictive forces on one site, anisotropy terms of Fe and R origin. Moreover a recent high temperature experiment on $Nd_2Fe_{14}B$ reveals that the paramagnetic susceptibility is a maximum for a direction about 45° from the *c*-axis [14].

In the light of our detailed results on the structures, we can propose a coherent sequence of the crystalline and magnetic transformations observed when lowering temperature.

Both the marked deviations from the *c*-axis of the paramagnetic easy direction and the symmetry lowering as evidenced by neutron diffraction should be related to the important high order CEF parameters of Nd and Ho.

- Above T_c, the rare earth local anisotropy leads the susceptibility to present a maximum in a direction tilted from the *c*-axis, within the (110) plane. If the iron anisotropy is weak enough or negligible, a low symmetry (SG: *C*2/*m* or *Cm*?) should appear.
- Below T_c and far above T_{SR}, the Fe magnetic moments order inducing — via the exchange forces J_{R-Fe} — the magnetic ordering of the R sublattices. The resulting direction of iron anisotropy is perpendicular to the iron layers (σ-type). The coupling forces lead to a rotation of the 4f orbitals and small shifts of neighbouring atoms.

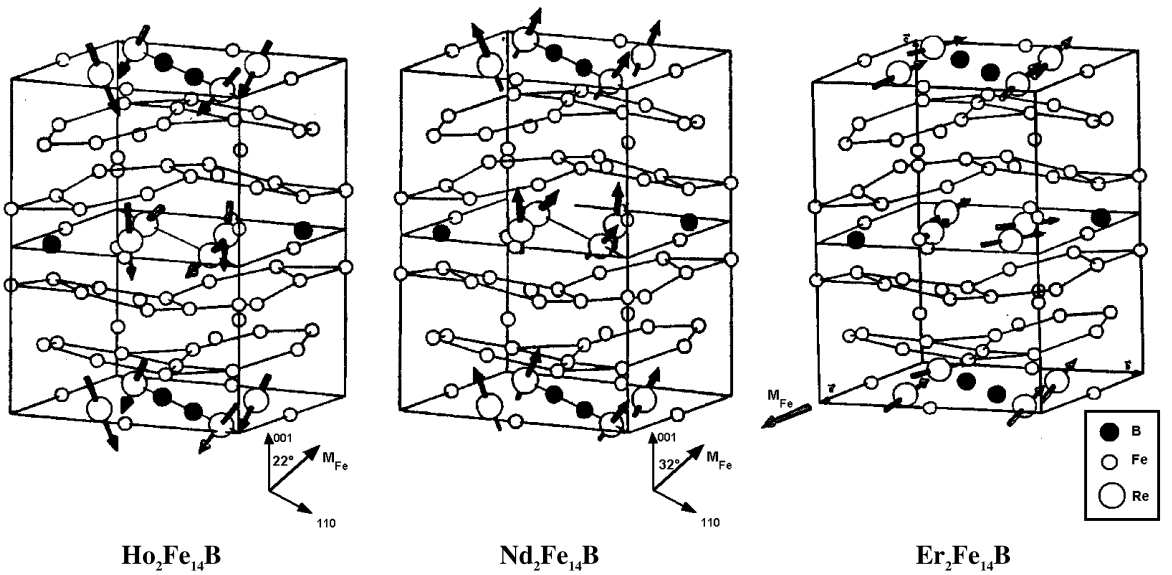

Fig. 3. Magnetic structures of $Ho_2Fe_{14}B$, $Nd_2Fe_{14}B$ and $Er_2Fe_{14}B$ at 20 K.

The crystal structure looks like the one retained up to now (SG: $P4_2/mnm$), however with small atom shifts as demonstrated by the forbidden diffraction reflections ($h0l$ and $0kl$).

- When temperature is lowered, the rare earth anisotropy terms markedly increase and progressively compete with the one of iron. The rare earth magnetic moments begin to form a fan arrangement since the two R sites exhibit rather different values of second order CEF parameters. At this point (e.g. 100 K for $Ho_2Fe_{14}B$), the monoclinic crystal structure clearly deviates from the prototype tetragonal arrangement. Simultaneously, negative exchange forces J_{R-R} induce a net distortion of the magnetic structure with the loss of the symmetry centre (SG: Cm'). Then the rotation of easy direction within the (110) plane starts ($T_{SR}=58$ K for $Ho_2Fe_{14}B$) as a compromise between the CEF parameter set on the two different R sites.

$Er_2Fe_{14}B$ is orthorhombic immediately below the first order SRT ($\approx$330 K, SG: $Pnn2$). The R moments exhibit a fan structure apart from the (100) plane as the result of J_{R-Fe} coupling forces, different strength of CEF parameters on the two R sites, and because of negative J_{R-R} exchange force. As for Ho and Nd, the latter coupling induce the loss of the symmetry centre.

Likely, the other so-called planar compounds exhibit similar features in their crystal structures (e.g. Sm, Tm, and Yb) as driven by negative second order CEF parameters. Since the effects of iron axial anisotropy are counterbalanced by those of the J_{R-Fe} exchange forces, some deviations from collinearity within the iron sublattices can be suspected. Recent computing based on such a model appears compatible with the neutron diffraction data, leading to lower values for the Debye–Waller terms.

This critical analysis of the thermal behaviour of crystalline and magnetic structures allows to develop a more detailed picture fully consistent with the spin reorientation process of the $R_2Fe_{14}B$ series.

References

[1] C.B. Shoemaker, D.P. Shoemaker, R. Fruchart, Acta Crystallogr. C40 (1984) 1665.

[2] D. Givord, H.S. Li, J.M. Moreau, Solid State Commun. 50 (1984) 497.

[3] J.M.D. Coey, H.S. Li, J.P. Gavigan, J.M. Cadogan, B.P. Hu, in: I.V. Mitchell (Ed.), Concerted European Action on Magnets, 1989, pp. 76–97.

[4] C.A. Dwiggins, Acta Crystallogr. A31 (1975) 395.

[5] D.I. Garber, R.R. Kinsey, in: 3rd Edition, BNL 325, National Neutron Cross Section Center, B.N.L, Upton, New-York 11973, 1976.

[6] P. Becker, P. Coppens, Acta Crystallogr. A30 (1974) 129.

[7] V.F. Sears, Atomic Energy of Canada Limited Report, AECL 8490, 1984.

[8] P.J. Brown, in: International Tables for Crystallography, Kluwer Academic, 1992, pp. C391–399, ILL Internal Report, SP 88BR5016, 1988.

[9] P. Wolfers, J. Appl. Crystallogr. 23 (1990) 554–557.

[10] P. Wolfers, S. Miraglia, D. Fruchart, S. Hirosawa, M. Sagawa, J. Bartolomé, J. Pannetier, J. Less-Common Metals 162 (1990) 237–249.

[11] D. Fruchart, S. Miraglia, S. Obbade, R. Verhoef, P. Wolfers, Physica B 180–181 (1992) 578–580.

[12] P. Wolfers, S. Obbade, D. Fruchart, R. Verhoef, J. Alloys Comp. 242 (1996) 74–79.

[13] S. Obbade, P. Wolfers, D. Fruchart, R. Argoud, J. Muller, E. Palacios, J. Alloys Comp. 242 (1996) 80–84.

[14] P. de Rango, private communication.